Hindawi
Shock and Vibration
Volume 2023, Article ID 3828501, 11 pages
https://doi.org/10.1155/2023/3828501

Research Article

Design and Test of Quad-Bundle Spacer Damper Based on a New Rubber Structure

Zhenbing Zhao,[1] **Bin Liu**,[1] **Shengchun Liu**,[2] **and Dachuan Zhang**[3]

[1]*School of Electrical and Electronic Engineering, North China Electric Power University, Baoding 071003, China*
[2]*China Electric Power Research Institute, Beijing 102401, China*
[3]*Shenzhen Jiyun Technology Co. Ltd, Shenzhen 518000, China*

Correspondence should be addressed to Zhenbing Zhao; zhaozhenbing@ncepu.edu.cn

Received 14 December 2022; Revised 12 March 2023; Accepted 13 March 2023; Published 21 March 2023

Academic Editor: R. Luo

Aiming at improving the handling efficiency and acquiring the satisfactory antivibration effect and damping performance, a quad-bundle spacer damper of 500 kV extra high voltage transmission lines was designed and developed based on a new rubber structure. Firstly, a mathematical vibration model of the spacer damper was constructed, and the structures of the defect-prone parts of the spacer damper were analyzed. Then, the structure was optimized based on the defect analysis, the clamp with fast installation as well as removal and the damper joint with superior performance were designed. On this basis, a new quad-bundle spacer damper was developed. Last but not least, the handling efficiency of the new quad-bundle spacer damper was evaluated, and performance tests were conducted according to the IEC standards. The evaluation and test results show that the handling efficiency, antivibration effect, and damping performance of the new quad-bundle spacer damper are significantly improved compared with those of the regular quad-bundle spacer damper, which provides a guarantee for the safe operation of 500 kV extra high voltage transmission lines.

1. Introduction

As an important part of the transregional electric energy transmission network in China, the safe operation of 500 kV extra high voltage transmission lines is of great significance to energy delivery [1]. The mutual whipping of bundle conductors caused by high winds and icing is one of the main threats [2], and the most common and effective way to deal with it is the installation of the quad-bundle spacer. The quad-bundle spacer inhibits the mutual whipping of bundle conductors by controlling the distance between them, which has a certain damping effect on breeze vibration and subspan oscillation [3–5]. However, as the operating time grows, some problems such as functional failure, dislodgement, and fracture [6] also emerge in its components. Besides, the installation and replacement of the quad-bundle spacer are carried out at high altitude, which makes the operation difficult and the handling efficiency quite low. Therefore, the analysis and optimization on the mechanical structure and installation layout of the quad-bundle spacer [7–15] have become an area of research focus.

Currently, numerous studies have focused on the finite element analysis and numerical simulation of spacer structures and layouts. Kubelwa et al. [7] proposed a sensitivity assessment method for damping characteristics based on the tests of frequency and force displacement response of a multiclass spacer damper, which compensates for the deficiencies of the relevant IEC standards in frequency response analysis. Fu et al. [8] proposed a new spacer damper structure and constructed a finite element model of the transmission line-spacer system to analyze the wind load response, and the results showed that the new structure can effectively control the conductor span vibration. Hanneman et al. [9] compared the bending strains of the different arms of the spacer damper in aeolian

vibration tests and subspan oscillation tests, and the results showed that the bending strains were concentrated at the joints of the clamps and damper joints. Kubelwa et al. [10] developed a mathematical model for the aeolian vibration of the quad-bundle spacer based on the Euler–Lagrange formalism and evaluated the performance of the model in wind energy consumption by conducting a test. Xu et al. [11] developed a new viscoelastic damper, and the numerical analysis results showed that it has high damping characteristics, good energy dissipation ability, and an antitilt effect. Mou et al. [12] investigated the arrangement scheme of the octuple bundle ice-covered spacer damper by aerodynamic simulation and finite element analysis and proposed an optimal installation scheme to control the line flyover. However, a lot of idealized assumptions were made in modelling and calculating when using the finite element analysis and numerical simulation, which makes the obtained results hard to be confirmed and applied in realistic scenarios.

Some studies have focused on the analysis of the failure mechanism of the quad-bundle spacer. Wu et al. [13] found that the quad-bundle spacer has the problems of bulky installation tools, a complicated installation process, and low installation efficiency. They proposed the design idea of quad-bundle spacer installation robot based on the existing installation tools. Zhao et al. found that the failure of the damping structure is an important factor leading to the defects of the quad-bundle spacer and line oscillation. Based on this, they put forward the governance measure of shortening the spacer bar arrangement spacing in [14]. Zhu [15] analyzed the phenomenon of spacer clamp falling off and the transmission line wear, and the results showed that the poor antivibration effect of the spacer was the main reason. Based on this, they proposed to improve the clamp rubber structure. In the research study given above, scholars have analyzed and explored the defects existing in quad-bundle spacers. In general, the quad-bundle spacers have three obvious deficiencies caused by the structural design. First, the complicated structure of the clamp leads to tedious installation. Second, the failure of the damping structure causes clamp off and line oscillation. Third, the line wear caused by the insufficient antivibration effect is also worthy of attention.

It is an important means to enhance the service life of the spacer and improve the safety level of the transmission line operation by digging deeper into the spacer failure mechanism and structural deficiencies and optimizing the design. At present, most of the studies are inclined towards numerical simulation and finite element analysis. There are few studies on the analysis and optimization of specific deficiencies of the quad-bundle spacer, and fewer relevant tests can be found. From the perspective of engineering practice, the function and performance of the quad-bundle spacer still have great room for improvement.

Based on the existing research, we aimed to improve the handling efficiency, antivibration effect, and damping performance of the quad-bundle spacer damper. A vibration mathematical model of the spacer damper was built, and the spacer operation and maintenance data were utilized and combined to analyze the deficiencies of the clamps and damper joints of the regular quad-bundle spacer damper so as to optimize the design of the clamp, damper joint, and frame plate. A new quad-bundle spacer damper was developed, and the handling efficiency, antivibration effect, and damping performance were evaluated and tested.

2. Mathematical Model and Structural Analysis

2.1. Mathematical Model of Quad-Bundle Spacer Damper. As shown in Figure 1(a), when the bundle conductor vibrates, the vibration is transferred to the clamp. The damping joint at the end of the clamp absorbs and consumes the vibration energy through the relative motion between the rubber damping components and the frame plate, so the ability of the spacer damper to suppress the vibration of the conductor is related to its vibrational energy consumption in a single vibration cycle [16]. Like most of motion modelling methods of [17, 18], a single bundle conductor, a single clamp, and a frame plate are selected as a vibration system to establish the spacer equation, assuming that the frame plate is rigidly clamped and ignoring the torsional stiffness of the bundle conductor itself. The simplified model is shown in Figure 1(b), where x_c is the instantaneous amplitude of the clamp, x_f is the instantaneous amplitude of the frame plate, k_t is the dynamic torsional stiffness of the vibration system damping structure, and h_t is the dynamic damping constant of the damping structure.

The motion equation of the vibration system is shown in equation (1), where m is the total mass of the vibrating system, the second-order and first-order derivatives of x_f with respect to time are denoted as the instantaneous acceleration and instantaneous velocity of the frame plate, and the first-order derivatives of x_c is the instantaneous velocity of the clamp. This equation of motion characterizes the vibration system shown in Figure 1(a), where there is relative motion between the clamp and the rigid frame plate.

$$m\frac{\mathrm{d}^2x_f}{\mathrm{d}t^2} + h_t\left(\frac{\mathrm{d}x_f}{\mathrm{d}t} - \frac{\mathrm{d}x_c}{\mathrm{d}t}\right) + k_t\left(x_f - x_c\right) = 0. \tag{1}$$

First, the simple case that both the clamp and the frame plate are in sinusoidal vibration is considered, as shown in equation (2). Here, A_f and A_c are the peak displacements, w is the vibration angular frequency, and $e^{j\theta}$ denotes the displacement decay factor after the damper joint.

$$\begin{cases} x_f = A_f e^{\mathrm{j}wt} e^{j\theta}, \\ x_c = A_c e^{\mathrm{j}wt}. \end{cases} \tag{2}$$

By substituting equation (2) into (1) and simplifying, the frame plate displacement x_f can be transformed into

$$x_f = \frac{k_t + jh_t w}{k_t - m_r w^2 + jh_t w} x_c, \tag{3}$$

where $F = ma$, and the combined force F acting on the system is obtained, as shown in equation (4).

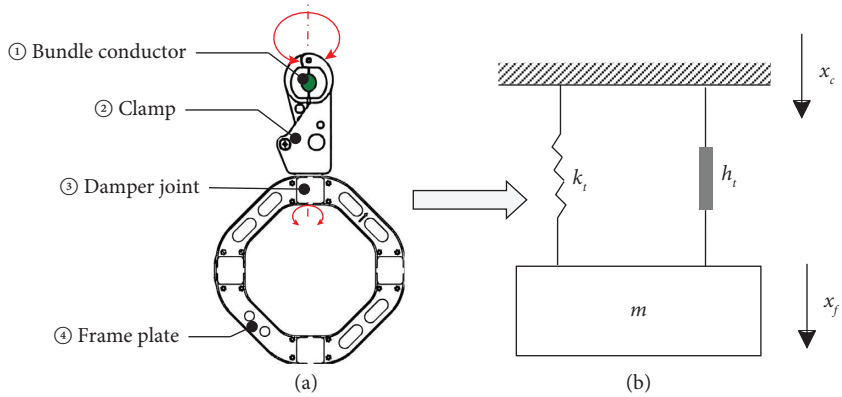

FIGURE 1: Schematic diagram of vibration transfer and vibration system equivalence model: (a) vibration transfer process and (b) vibration system equivalence model.

$$F = -m\frac{d^2x_f}{dt^2} = \frac{-jmh_tw^3 + \left(k_t^2 - mk_tw^2 + h_t^2w^2\right)}{\left(k_t - mw^2\right)^2 + \left(h_tw\right)^2} mw^2A_ce^{jwt}. \tag{4}$$

The energy is expressed by equation (5), where V is the instantaneous velocity of the clamp. The angle between force and velocity can be deduced from F, so the system energy dissipation E in a single vibration cycle is expressed by equation (6).

$$E = \int_0^T \overline{F} \cdot \overline{V} dt, \tag{5}$$

$$E = \frac{-\pi {A_c}^2 {m_r}^2 h_t w^5}{\left(k_t^2 - m_r k_t w^2 + h_t^2 w^2\right)^2 + \left(m_r h_t w^3\right)^2}. \tag{6}$$

When the spacer damper-bundle conductor system is in stable vibration, the vibration amplitude is small, the vibration frequency is high, the individual vibration cycle is short, and the differences between the vibration amplitudes and the vibration frequencies of the adjacent clamps are small. Therefore, when estimating the overall energy consumption of the spacer within a single vibration cycle, the peak amplitude of vibration of all clamps A_c and the angular frequency of vibration w are approximately equal. The overall energy consumption of the spacer is the product of the aforementioned system energy consumption and the number of clamps. In actual scenarios, the composite clamp vibration equation can be characterized in a vector sum form, which consists of multiple vibration equations with different directions, different frequencies w, and different peak amplitudes A_c. Similarly, the frame vibration equation can be characterized into a vector sum form, consisting of multiple clamp composite vibrations under the action of different displacement attenuation factors. The multiple clamp composite vibration equations and the frame composite vibration equations can then be substituted into the above model in turn to estimate the overall energy consumption of the spacer. In a single vibration cycle, the more vibration energy of the bundle conductor the spacer consumes, the smaller the overall vibration amplitude of the spacer damper-bundle conductor system. To sum up, the antivibration effect can be characterized by the vibration energy consumed by the spacer in a single vibration cycle.

2.2. Damper Spacer Structural Analysis. Based on the statistical data of spacer faults on 500 kV lines and above in a province in eastern China [15], the spacer damage distribution is listed in Table 1. It can be seen that the fault types that occur during the spacer operation are mainly missing bolts or cotter pins and fracture and breakage, of which fracture and breakage are serious faults that can easily cause line breakage and other accidents. In terms of the spacer structure, the faults are mainly concentrated in the clamp and the damper joint.

As shown in Figure 2(a), the clamp of a regular quad-bundle spacer damper consists of a clamp gland, clamp body, and rubber pad. The body of the clamp is provided with assembly holes, and the pin provides pressure on the clamp gland to hold the bundle conductor within the rubber pads.

Figure 2(b) shows the fixed structure of the clamp. The cotter pin connects to the pin body through the pin end of the small hole, and the pin head is often installed with one or two pieces of shims to increase the force area and reduce the contact force so as to prevent the pin from coming off. There are two deficiencies in the operation of this clamp structure. One is that the service life of the cotter pin is much shorter than that of the pin spindle, and its protection effect is not obvious. Since the cotter pin itself has a low load carrying capacity and is exposed to the outside of the clamp, it is easy for the cotter pin to corrode and fall off under long-term vibration or humid environment. The other is that the clamp handling efficiency is not satisfactory. In fact, the spacer installation as well as removal in transmission line maintenance is generally an overhead live-line operation, and the maintenance personnel need to complete the cotter pin removal and pin spindle extraction operations through the

Table 1: Statistical data of the damage of spacer damper.

Fault type	Number	Percentage
Missing bolt or missing cotter pin	340	57.14
Fracture and breakage	145	24.3
Loose rubber pads	46	7.7
Dislodged clamps	28	4.7
Displacement	25	4.2
Others	11	2.2

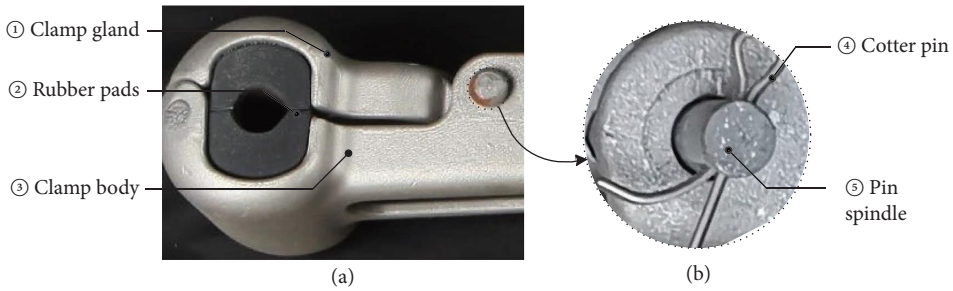

Figure 2: Structure of the regular spacer damper clamp: (a) clamp component composition and (b) structure composition of the clamp installation part.

alternate use of multiple tools. Due to the small working space, it is difficult to alternately use tools, and the disassembly and replacement of spacers take a long time. In addition, there exists installation irregularities due to the installation difficulty, personnel operation level, and other factors that lead to cotter pin installation irregularities and a reduction in the service life of the clamp.

As shown in Figure 3(a), the damper joint of regular quad-bundle spacer damper is located at the end of the clamp and consists of damping blocks, star-shaped shaft, bolt assembly hole, and damping joint enclosure. The damping blocks are viscoelastic, and their elasticity is available to the spacer to restrain the stiffness of the bundle conductor, while their viscosity is used to consume the damping of the vibration energy. The star-shaped shaft with damping joint enclosure acts as a rigid restraint to avoid excessive amplitude conductor vibration. The assembly holes are bolted to the clamp and frame plate, maintaining the overall stability.

Figure 3(b) shows the fixed structure of the damper joint. The shaft projection and the frame plate recess cooperate with each other, and the fastening bolt passes through the assembly hole with the spacer and nut connecting the frame plate to the clamp. This damper joint structure has two drawbacks in operation. One is that the connection between the star-shaped shaft and the frame plate is a rigid metal contact, which has poor wear resistance. In the event of significant bundle conductor vibration, the star shaft projection and the frame plate groove collide directly with the rigid metal, causing groove rupture and wear. Secondly, the vibration energy in the linear direction cannot be absorbed by the damping blocks. In this damper joint structure, the star shaft is directly connected to the frame plate recess without a movement margin in the parallelogram direction, leading to the accumulation of vibration energy in this direction and the wear of the star shaft and the frame plate recess.

3. New Quad-Bundle Spacer Damper

The new quad-bundle spacer damper is designed based on the structure of the abovementioned spacer damper. To improve the damping performance, antivibration effect, and installation efficiency of the spacer, from optimization angle of the three major components, i.e., clamp, damping joint, and frame plate, the design was then carried out. The structure of the new quad-bundle spacer damper is shown in Figure 4. It mainly consists of a self-locking clamp, damper joint, and frame plate. The self-locking clamp uses a spring-loaded latch plate to achieve rapid installation as well as removal of the spacer damper. The damping joint improves the ability to withstand bundle conductor movement through the combination of an energy-absorbing rubber sleeve and telescopic rod. The frame plate uses a composite plate and antiloosening bolts to ensure the overall stability of the spacer damper.

3.1. Clamp Design. The clamp has the function of holding the bundle conductor, which is the basis for the spacer to play the role of vibration and energy dissipation. They need to provide a stable and continuous tightening force to the bundle conductor, provided that the conductor is not damaged.

The optimized structure of the quad-bundle spacer damper clamp is shown in Figure 5(a). The overall structure of the clamp is still composed of the clamp gland, body of the clamp body, and rubber pad. The clamp fixing structure is optimized in order to shorten the clamp operation time and improve the handling efficiency.

As shown in Figure 5(b), the clamp fixing structure consists of a clamp gland, a latch, a limit slot, and a spring. When the clamp is not installed, the clamp gland is on top of the latch and the spring is in a no-load state. When the clamp is installed, the clamp gland is pressed down by an

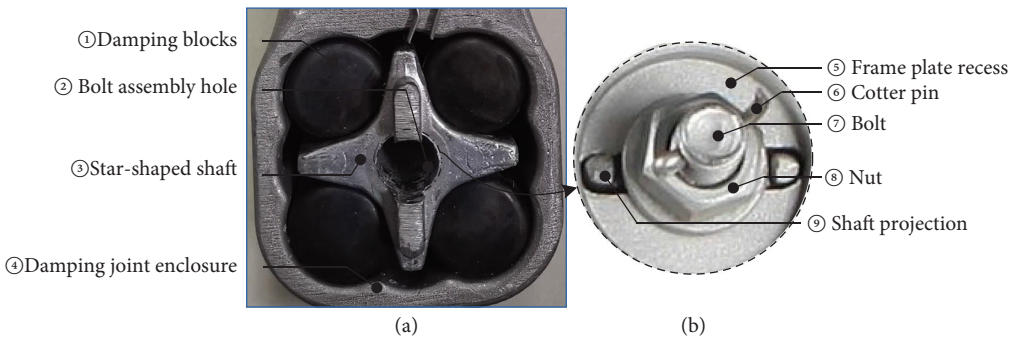

Figure 3: Damper joint structure of the regular spacer damper: (a) damper joint component composition and (b) structure composition of damper joint fixation part.

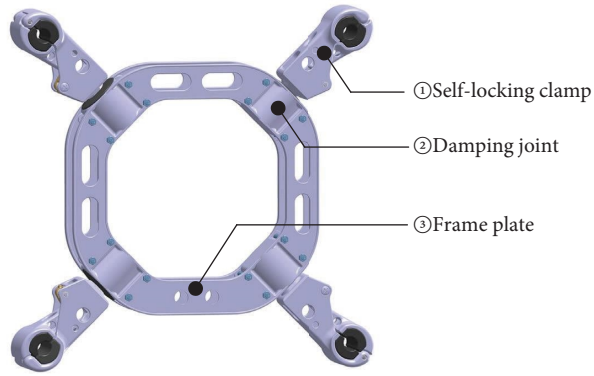

Figure 4: Structure of the new type of the quad-bundle spacer damper.

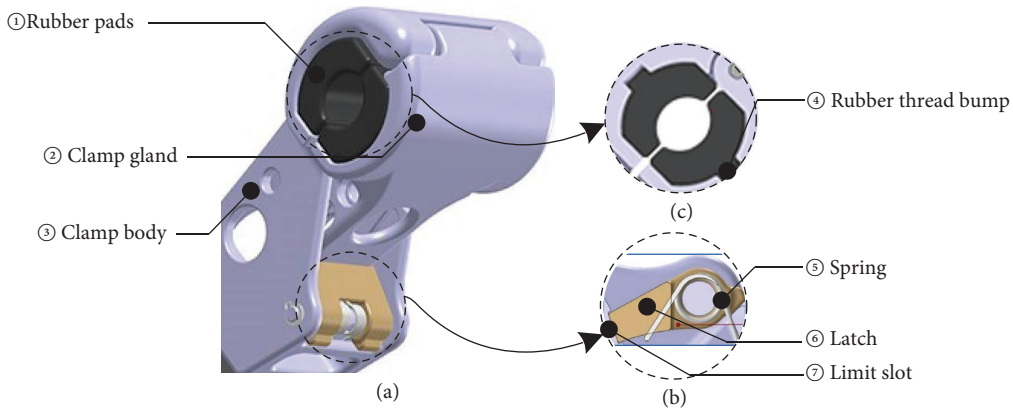

Figure 5: Clamp structure of the new quad-bundle spacer damper: (a) clamp component composition, (b) structure composition of clamp fixation part, and (c) rubber mat structure cross section.

installation tool, as shown in Figure 6, thereby driving the latch down into the limit slot. During this process, the spring changes from a nonload state to a load state, and the elastic deformation of the spring causes the latch to press against the outer projection of the limit slot. It allows the latch to exert inward pressure on the gland of the clamp, thus realizing the function of fastening the bundle conductor. When the clamp is dismantled, as the limit slot is on the sloping surface of the clamp gland, the inner side of the limit slot is lower than the outer side. Using the disassembly tool, shown in Figure 6, to push the tongue inwards into the limit slot, the clamp gland can be popped out, and the clamp is restored to an uninstalled state.

In addition, as shown in Figure 5(c), the new quad-bundle spacer damper clamp has been structurally optimized with a new cylindrical projection at the bottom of the rubber pad and a new limit slot in the clamp plate to prevent the rubber pad from falling off.

Figure 6: Sketch of installation and disassembly tool.

3.2. Damper Joint Design. The damper joint is the connecting structure between the spacer damper clamp and the frame plate, whose performance is determined by the mechanical structure of the joint and the viscoelastic properties of the damping rubber parts. It not only needs good damping and energy dissipation characteristics but also needs to provide sufficient movement margin for the clamps to suppress small amplitude breeze vibrations and subgrade oscillations and prevent the damage to the bundle conductors from large amplitude oscillations.

The optimized structural design of the damper joint of the new quad-bundle spacer damper is shown in Figure 7(a). In response to the main deficiencies of regular damper joints, the new quad-bundle spacer damper is designed with a new damping rubber structure so as to improve the damping performance of the spacer bar and the activity margin in all directions. The damper joint consists of the energy-absorbing rubber sleeves, a retractor bracket, and a retractor ejector. Figure 7(b) shows the structure of the energy-absorbing rubber sleeve, designed as a hollow rubber ring. It consists of two parts. The outer rubber sleeve is fixed to the retractor holder and ends in the retractor ejector, while the inner rubber sleeve is embedded inside the damping joint and is flexibly connected to the retractor ejector.

When the bundle conductor is blown by the wind, the vibration is transferred from the clamp to the retractor ejector of the damping joint, and then the relative movement among the retractor ejector, energy-absorbing rubber sleeve, and frame plate absorbs and consumes the vibration energy. According to the spacer test standard [19], the relative motion of the bundle conductor with the addition of the spacer damper can be decomposed into horizontal relative motion, vertical relative motion, longitudinal relative motion, and conical relative motion around the connection point. For the horizontal relative motion, the internal structure changes of the damping joint are shown in Figure 8(a), and the retractor ejector dissipates the vibration by squeezing the inner and outer rubber sleeves back and forth in parallel. For the vertical relative motion, the internal structure changes of the damping joint are shown in Figure 8(b), and the retractor ejector dissipates the vibration by squeezing the upper and lower sides of the internal and external rubber sleeves back and forth. For the longitudinal relative motion, the internal structure changes of the damping joint are shown in Figure 8(c), where the retractor ejector dissipates the vibration by squeezing the internal rubber sleeve and the left and right sides of the external rubber sleeves back and forth. For the conical relative motion around the connection point, the retractor head is embedded in the damping joint, which does not restrict the movement of the clamp and allows for 360 degrees of unobstructed conical motion and a certain angle of circumferential twisting of the entire clamp. As a result, the damper joint allows for sufficient movement in any direction in relation to the clamp, which is significantly better in all directions than a regular damper joint. In addition, the double sleeve design avoids direct rigid contact between the damper joint and the frame plate so as to increase the service life of the internal parts of the damper joint.

3.3. Frame Plate Design. The frame plate maintains the overall stability of the spacer by fixing the damper joints. The transmission and suppression of vibration by the damper joints make the mechanical load of the frame plate more concentrated, so the frame plate must have good mechanical strength.

As shown in Figure 9(a), the frame plate of the new quad-bundle spacer damper is designed with reference to the regular spacer damper using a composite double plate structure. The damping joint fixing structure is optimized on the basis of the original frame plate. It consists of a fastening bolt and two round the hole nuts. The fastening bolt is left with a forward coarse thread and a reverse fine thread, the coarse round the hole nut with the bolt provides fastening force for the upper and lower two frame plates, and the fine round the hole nut with the bolt blocks the coarse. Compared to the regular spacer, the fine nut has better corrosion resistance and load-bearing properties than the cotter pin.

In addition, as shown in Figure 9(a), the new quad-bundle spacer damper moves the fastening bolts from the center of the damper joint to the four corners, and it provides an active cavity to isolate the damping components from the external environment. In this way, the sealing property of the damping rubber parts is ensured, which can prevent the aging of the damping rubber components caused by the complex external environment. It can increase the flexibility of the damper joint and prolong the service life of the damping rubber components and maintain the damper efficiency during long-term operation.

4. Performance Analysis

Through extensively investigating the material and dimensional parameters of regular quad-bundle spacers damper, the new quad-bundle spacer damper was manufactured. The clamp and frame plate are made of aluminum alloy, the energy-absorbing rubber sleeve is made of synthetic silicone rubber, and the rest are made of hot-platedlead-zinc. The overall weight is slightly lighter than the regular quad-bundle spacer damper, and the manufacturing cost is comparable to the regular one. The physical diagram of the new quad-bundle spacer damper is shown in Figure 10(a), the dimensional diagram is shown in Figure 10(b), and the main parameters are listed in Table 2.

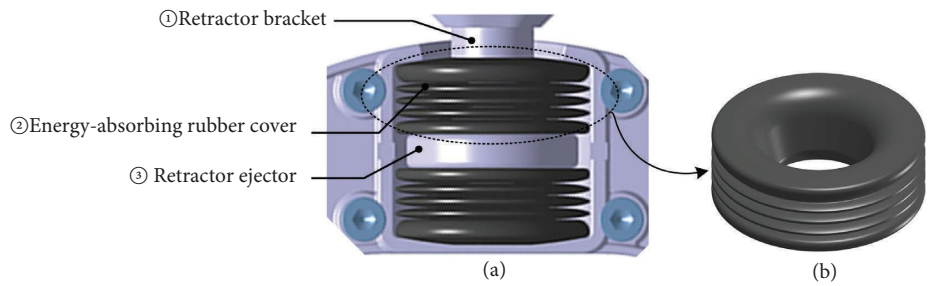

Figure 7: Damping joint structure of the new quad-bundle spacer damper: (a) damping joint component composition and (b) energy-absorbing rubber sleeve structure.

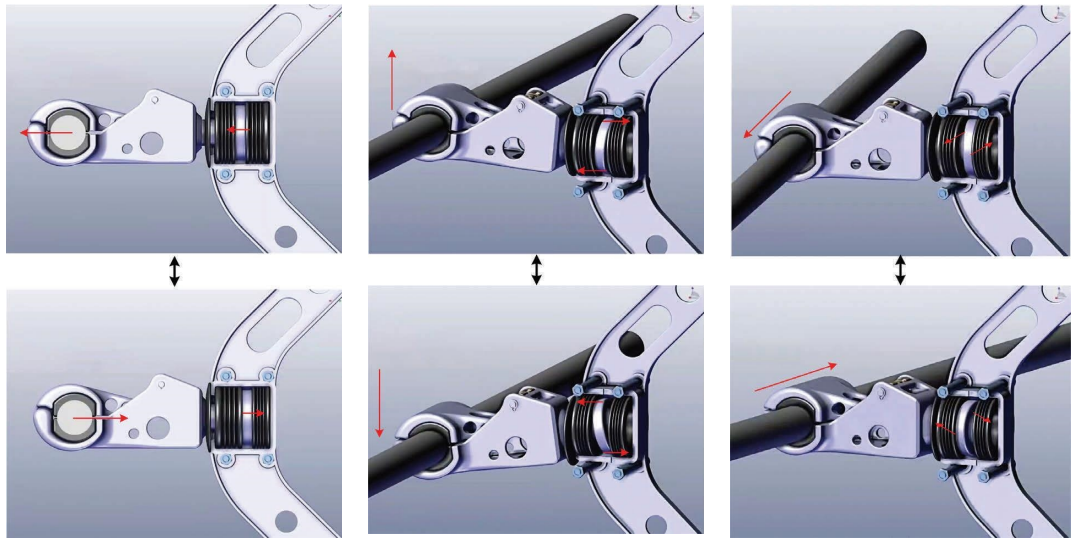

Figure 8: Schematic diagram of structural changes inside the damping joint when the relative motion of the bundle conductor occurs: (a) horizontal relative motion, (b) vertical relative motion, and (c) longitudinal relative motion.

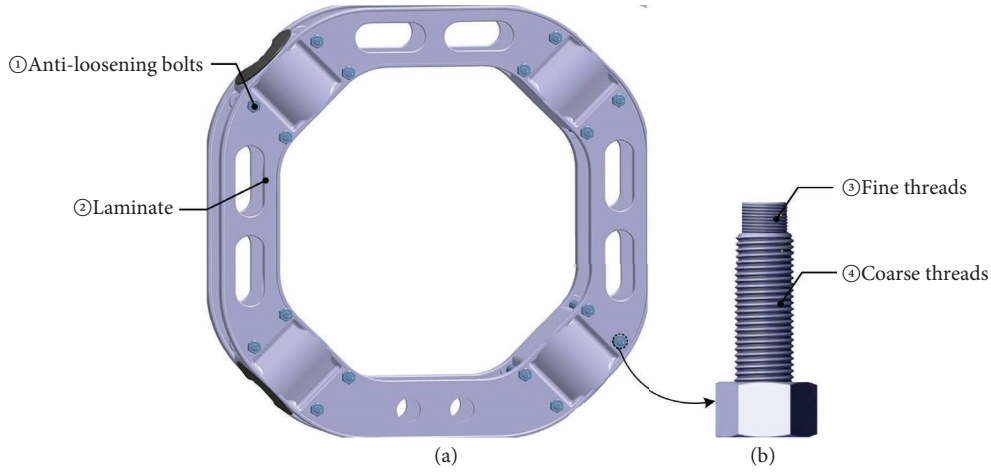

Figure 9: Frame plate structure of the new quad-bundle spacer damper: (a) frame plate component composition and (b) antiloosening bolt structure.

4.1. Handling Efficiency Analysis. To verify the improvement in handling efficiency, the installation process of the new quad-bundle spacer damper clamp is given in Figure 11(a). The installation of the self-locking cable clamp only requires an installation tool to press the cable clamp gland in the direction of the red arrow so that the latch can enter the limit

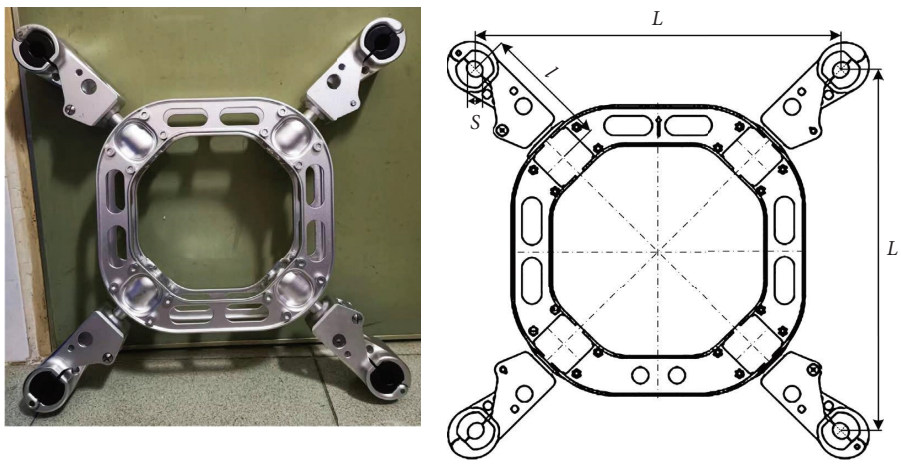

(a) (b)

Figure 10: The new quad-bundle spacer damper physical and dimensional diagram: (a) physical diagram and (b) dimensional diagram.

Table 2: Parameters of the new type of quad-bundle spacer damper.

Parameters	Parameter description	Values
S	Applicable wire diameter	23.0 mm–24.5 mm
L	Bundle spacing	450 mm
L	Clamp length	160 mm
M	Weight	6.905 kg

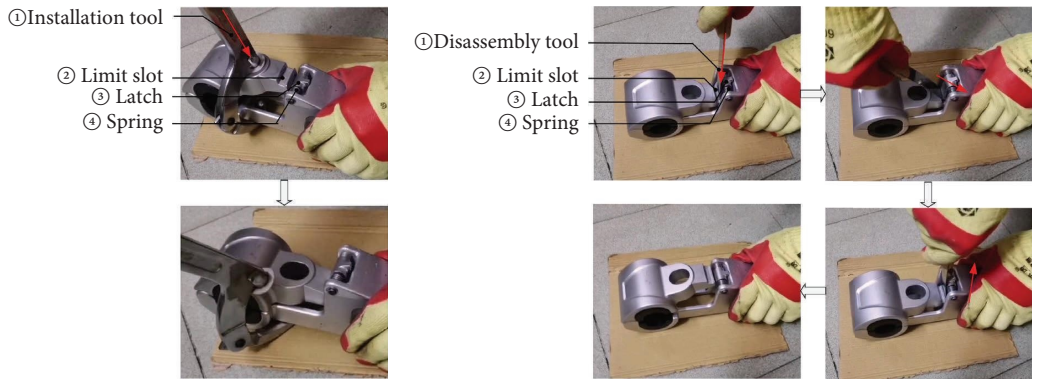

(a) (b)

Figure 11: Installation and disassembly process of the new quad-bundle spacer damper clamp: (a) installation process and (b) disassembly process.

slot. In contrast, the traditional clamp requires three steps, that is, pretightening the clamp gland and the bundle conductor, threading the pin through the assembly hole, and installing the cotter pin or tightening the nut during installation. The one-step operation improvement of new quad-bundle spacer damper clamp saves much installation time.

In Figure 11(b), the disassembly process of the new quad-bundle spacer damper is demonstrated. During the disassembly, the putty knife is inserted diagonally inward into the limit slot, then the latch is pushed out of the limit slot, and the putty knife is pulled out to complete the disassembly. The traditional clamp requires three steps to remove the cotter pin or the fastening bolt, that is, the pin removal, the clamp gland separation, and the bundle conductor splitting. The new quad-bundle spacer damper saves these operations and optimizes the operation process, improving the uninstallation efficiency to a certain extent.

4.2. Analysis of Damping and Antivibration Properties. In order to verify the antivibration effect and the improvement of the damping performance of the new quad-bundle spacer damper, several performance tests of the new quad-bundle spacer damper were carried out according to the IEC standard [19].

According to the IEC standard "Overhead lines requirements and tests for spacers" [19], the damping method was used for the characterization of elastic and damping properties of spacer. The test was performed at room temperature (20 ± 5°C), and the specimens were placed at room temperature for at least three hours before the test. The spacer frame was fixed, and a weight was hung on one of the clamps so that the natural swaying frequency was between 1 Hz and 2 Hz. Then, the clamps were shifted at a certain angle and the pressure was suddenly released after one minute. The free decaying waveform of the clamp was recorded, and the amplitudes Y_0, Y_1, Y_2, and Y_3 in four decay periods were measured. The logarithmic decay rate δ_i was calculated by equation (7). The average value of the logarithmic decay rate $\widetilde{\delta}_i$ is taken as the final result of several tests.

$$\delta_i = \ln\left[\frac{1}{2}\left(\frac{Y_0}{Y_2} + \frac{Y_1}{Y_3}\right)\right]. \tag{7}$$

The displacement decay curve of the spacer damper clamp is shown in Figure 12. The initial amplitude Y_0 was 116.00 mm, which decayed to approximately 75.80 mm after the first decay period, 42.54 mm after the second period, and 36.02 mm after the third period. The average logarithmic decay rate $\widetilde{\delta}_i$ was approximately 0.88 after several test measurements.

Based on the stiffness-damping method for the characterization of the elastic and damping properties of spacers in the IEC standard "Overhead lines requirements and tests for spacers" [19], the tests were performed at room temperature (20 ± 5°C) and the specimen was placed at room temperature for at least three hours before the test. The frame of the spacer damper was fixed, and a sinusoidal excitation was applied to the clamp along the vertical clamp direction so that its instantaneous deflection angle φ could satisfy the sinusoidal distribution shown in equation (8). Here, Φ is the peak deflection angle selected for the current measurement.

$$\varphi = \Phi \sin \omega t. \tag{8}$$

In the process of measuring the angle Φ, the peak value of the oscillating force F_m was measured and the phase angle between the force and the deflection angle was calculated from the closed hysteresis line formed by the deflection angle of the force and the force arm, as shown in equation (9). Here, l is the length of the force arm and E is the vibration energy consumed in a single sinusoidal vibration cycle.

$$\alpha = \arcsin\frac{E}{\pi l F_m \Phi}. \tag{9}$$

The torsional stiffness K_t and the damping constant H_t can be derived from the peak force F_m and the phase angle, as shown in the following equations:

$$K_t = \frac{F_m l \cos\alpha}{\Phi}, \tag{10}$$

$$H_t = K_t \tan\alpha. \tag{11}$$

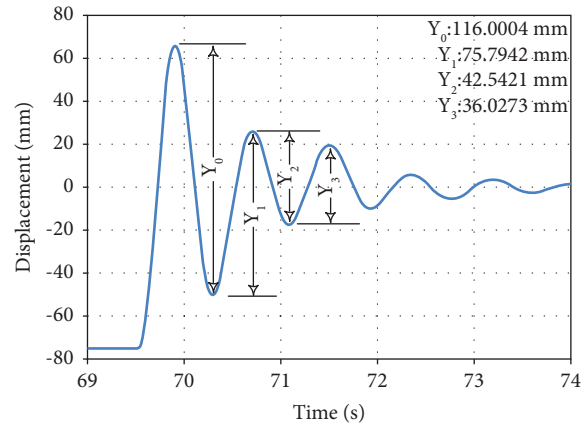

Figure 12: Displacement decay curve of the spacer damper clamp.

In order to reduce the test error, three stiffness-damping tests were conducted according to the aforementioned process, and the average values of torsional stiffness and damping constant were taken as the final result. The test data of the new quad-bundle spacer damper are listed in Table 3. After three measurements and averaging of the results, the torsional stiffness K_t of the new quad-bundle spacer damper was 239.56 $N*m$/rad and the damping constant H_t was 54.8 $N*m$/rad.

In order to comprehensively evaluate the damping performance and antivibration effect of the new quad-bundle spacer damper, the stiffness-damping method was utilized in the tests. The test results of a variety of regular quad-bundle spacer dampers [20] and the new quad-bundle spacer damper were selected for cross-contrast analysis. Specifically, the damping performance of the new quad-bundle spacer damper was evaluated by comparing their damping constant and their torsional stiffness, and the antivibration effect of the new quad-bundle spacer damper was assessed by comparing the vibration energy dissipation in a single cycle. The comparison results of torsional stiffness and damping constant measurements are shown in Figure 13(a). From the visualization of the results, it can be seen that the new quad-bundle spacer damper has a significant increase in both metrics over the regular quad-bundle spacer damper. Compared with the average level of the regular quad-bundle spacer, the torsional stiffness and damping constant of the new quad-bundle spacer damper were improved by about 25.6% and 36.5%. This indicates that the new quad-bundle spacer damper can provide more activity margins than regular ones, and its damping performance is also better.

The comparative results of energy consumption within a single vibration cycle are shown in Figure 13(b). The energy dissipation of a single clamp in a single vibration cycle was about 4.284 J, while the highest energy dissipation of a single clamp in a single vibration cycle was about 3.76 J in a variety of regular quad-bundle spacer dampers. In a single vibration cycle, the energy consumed by the new quad-bundle spacer damper was 1.8 times that of the average level. Therefore, it is more competitive than a regular spacer in terms of its antivibration effect.

Table 3: Test data of the new quad-bundle spacer damper.

	Parameters					K_t	H_t
	F_m	l	E	α	Φ		
1	242.58	160	4.060	0.23	0.16	236.27	54.99
2	249.36	160	4.572	0.22	0.16	242.79	56.88
3	245.3	160	4.224	0.23	0.16	239.62	52.55
Average	245.74	160	4.284	0.23	0.16	239.56	54.80

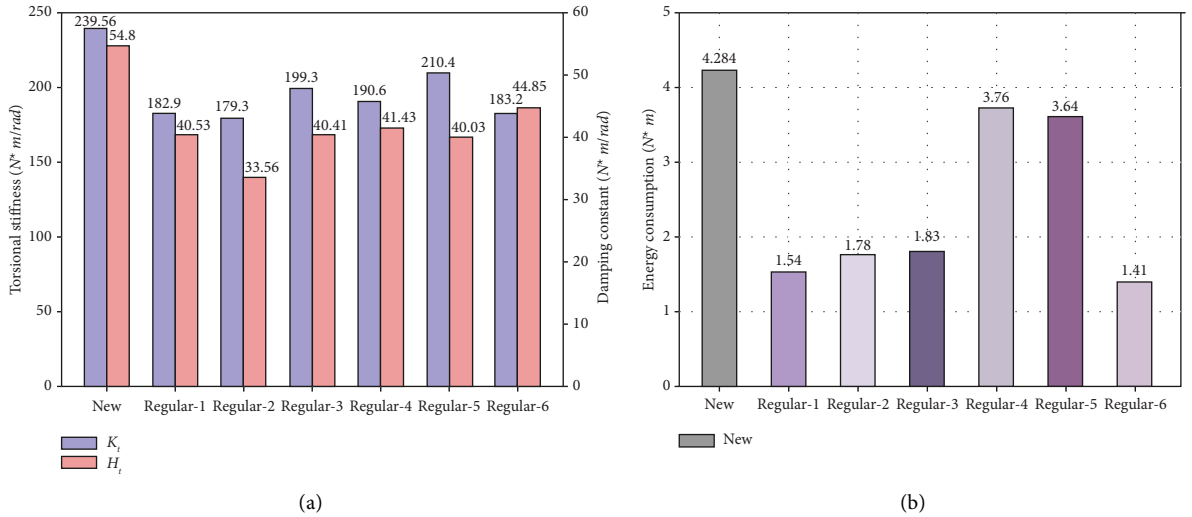

(a) (b)

Figure 13: Comparison of test results: (a) torsional stiffness and damping constant visualization comparison results and (b) energy consumption comparison visualization results.

5. Conclusions

In this paper, the structural deficiencies of regular spacer dampers were analyzed according to spacer operation and maintenance data, and a new quad-bundle spacer damper was developed by optimizing the design of the clamp fixing structure and damping structure. The effectiveness of the clamp structure and damping structure was proven by the evaluation of the installation as well as removal processes of the clamps and by testing the damping performance according to the IEC standards. Conclusions are drawn as follows:

(1) The clamp structure adopted in this paper greatly simplifies the installation as well as removal process, thus significantly improving its handling efficiency compared to that of the regular quad-bundle spacer damper.

(2) Compared with the average level of damping structure of the regular quad-bundle spacer, the torsional stiffness and damping constant of the damping structure adopted in this paper were improved by about 25.6% and 36.5%. Its energy dissipation was 1.8 times of the average level, showing better damping performance and antivibration effect.

Data Availability

The data used to support the findings of this study are included within the article.

Conflicts of Interest

The authors declare that they have no conflicts of interest.

Acknowledgments

This work was supported by the National Natural Science Foundation of China (project numbers 61871182 and U21A20486), the Funded Project for Innovative Graduates in Hebei Province of China (CXZZSS2023193), and the Natural Science Foundation of Hebei Province (project numbers F2020502009, F2021502008, and F2021502013).

References

[1] D. Q. Chen, X. H. Guo, P. Huang, and F. H. Li, "Safety distance analysis of 500kV transmission line tower UAV patrol inspection," *IEEE Letters on Electromagnetic Compatibility Practice and Applications*, vol. 2, no. 4, pp. 124–128, 2020.

[2] P. V. Hung, H. Yamaguchi, M. Isozaki, and J. H. Gull, "Large amplitude vibrations of long-span transmission lines with bundled conductors in gusty wind," *Journal of Wind Engineering and Industrial Aerodynamics*, vol. 126, pp. 48–59, 2014.

[3] M. Zhang, G. Zhao, L. Wang, and J. Li, "Wind-induced coupling vibration effects of high-voltage transmission tower-line systems," *Shock and Vibration*, vol. 2017, Article ID 1205976, 34 pages, 2017.

[4] G. Zhao and X. Rui, "A preliminary analysis on mechanical characteristics of transmission conductors in the vicinity of

suspension clamps," *IOP Conference Series: Earth and Environmental Science*, vol. 631, no. 1, Article ID 012095, 2021.

[5] H. Agarwal, S. Mukherjee, S. Chattaraj, M. I. Khan, and D. Prasad, "Development of quad spacer damper to suppress oscillation in 765 kV transmission line," in *Proceedings of the IEEE International Conference on Computing, Communication and Networking Technologies*, pp. 1–6, IEEE, Kharagpur, India, July 2020.

[6] F. Foti, L. Martinelli, and F. Perotti, "A parametric study on the structural damping of suspended cables," *Procedia Engineering*, vol. 199, pp. 140–145, 2017.

[7] Y. D. Kubelwa, A. G. Swanson, D. G. Dorrell, and K. O. Papailiou, "A comparative study on high-voltage spacer-damper performance and assessment: theory, experiments and analysis," *SAIEE Africa Research Journal*, vol. 110, no. 3, pp. 153–166, 2019.

[8] X. Fu, H.-N. Li, J.-X. Li, and P. Zhang, "A pounding spacer damper and its application on transmission line subjected to fluctuating wind load," *Structural Control and Health Monitoring*, vol. 24, no. 8, Article ID e1950, 2017.

[9] A. J. Hanneman, J. J. Olenik, and D. C. Sunkle, "Bending strain comparison on various spacer damper arms," in *Proceedings of the 2019 IEEE PES GTD Grand International Conference and Exposition Asia (GTD Asia)*, pp. 320–325, Bangkok, Thailand, March 2019.

[10] Y. D. Kubelwa, A. G. Swanson, K. O. Papailiou, and D. G. Dorrell, "On the euler-Lagrange formalism to compute power line bundle conductors subject to aeolian vibrations," *Mechanical Systems and Signal Processing*, vol. 163, Article ID 108099, 2022.

[11] Z. D. Xu, L. Z. Xu, and F. H. Xu, "Study on the iced quad-bundle transmission lines incorporated with viscoelastic antigalloping devices," *Journal of Dynamic Systems, Measurement, and Control*, vol. 137, no. 6, Article ID 061009, 2015.

[12] Z. Mou, B. Yan, H. Yang, K. Wu, C. Wu, and X. Yang, "Study on anti-galloping efficiency of rotary clamp spacers for eight bundle conductor line," *Cold Regions Science and Technology*, vol. 193, Article ID 103414, 2022.

[13] Z. Wu, Z. Jianqi, C. Haigen, and Z. Huang, "Development on robot installation using quad spacer damper," in *Proceedings of the International Conference on Artificial Intelligence, Virtual Reality, and Visualization (AIVRV 2021)*, vol. 12153, SPIE, Sanya, China, December 2021.

[14] J. Zhao, "Analysis of the damping failure of the spacer bar and the hinge pin falling off and exiting the overhead transmission line," *Inner Mongolia Electric Power Technology*, vol. 38, no. 05, pp. 25–29, 2020.

[15] D. Zhu, "Operation status analysis and optimization suggestions of multi split sub conductor spacer," in *Proceedings of the 2017 Excellent Proceedings of Zhejiang Electric Power Society*, Zhejiang, China, January 2017.

[16] S. Mukherjee, D. Prasad, M. I. Khan, P. Barua, and H. Agarwal, "Hexa spacer damper for vibration energy decaying of 765 kV transmission line," in *Proceedings of the 2019 Innovations in Power and Advanced Computing Technologies (I-PACT)*, pp. 1–6, Vellore, India, March 2019.

[17] J. Si, X. Rui, B. Liu, L. Zhou, and S. Liu, "Study on a new combined anti-galloping device for UHV overhead transmission lines," *IEEE Transactions on Power Delivery*, vol. 34, no. 6, pp. 2070–2078, 2019.

[18] C. Liu, D. Wang, and M. Hou, "A new type of damped spacer bar for suppressing sub-grade distance oscillation of transmission lines and its vibration damping effect analysis," *Chinese Journal of Electrical Engineering*, pp. 1–13, 2020.

[19] International Electrotechnical Commission, "Overhead lines - requirements and tests for spacers," International Electrotechnical Commission, London, UK, IEC 61854-2020, 2020.

[20] J. Zhao, Z. Jianli, Y. Baofeng et al., "Aeolian vibration model and experimental study on damping characteristics of damper spacers," in *Proceedings of the IEEE International Conference on Renewable Energy and Power Engineering*, pp. 175–179, IEEE, Beijing, China, October 2021.